

Development of a Low-Cost Sensor to Optimise the Use of Fertilisers in Irrigation Systems

Francisco Javier Diaz¹, Ali Ahmad¹, Sandra Viciano-Tudela¹, Lorena Parra¹, Sandra Sendra¹, Jaime Lloret^{1*}

¹Instituto de Investigación para la Gestión Integrada de Zonas Costeras, Universitat Politècnica de València, 46730 Grau de Gandia, Spain

Email: fjdiabla@doctor.upv.es, aahmad1@upv.es, svictud@upv.es, loparbo@doctor.upv.es, sansenco@upv.es, jlloret@dcom.upv.es

Abstract— Fertilizers are widely used in agriculture to ensure the availability of nutrients for crops. Sensors are being used to determine fertilizers concentration in precision agriculture systems. In this paper, we present a low-cost sensor for determining fertilizer concentration based on optical and electromagnetic sensors. The combination of sensors prevents the overestimation of fertilizers. Four Two-Coil Systems (TCSs) were compared to determine which offered the most suitable data for determining the fertilizer in the water. The number of spires of powered and induced coils of TCSs ranged from 20 to 80 spires. A single configuration using a light source and light receptor is proposed for the optical sensor. Six calibration samples were prepared to calibrate both the TCSs and the optical-based sensor. The calibration samples vary from 0 to 10 mL/L of fertilizer. Results indicate that TCS 2 b is the one that offers the most accurate results among the tested TCSs. The single regression model obtained with data from TCS 2 b was characterized by a correlation coefficient of 0.988. Finally, the data for both sensors are used in an ANN model to predict the fertilizer concentration of samples. The correctly classified cases were 100 %.

Keywords- Two-Coil System, copper coil, optical sensor, electromagnetic sensor, agriculture, artificial neural network.

I. INTRODUCTION

Soil fertility refers to the ability of soil to support and sustain plant growth. This ability is influenced by many factors, such as nutrient and minerals presence, soil texture, soil organic matter, pH amount of water and biomass [1] [2]. Soil minerals usually cover up half of the soil volume, and their composition varies among different types of soils, changing their chemical composition and physical properties. At the same time, the mineral composition is affected by life forms present in the environment, modifying them. Moreover, the organic matter, complementary to soil minerals and fused together, makes up the solid phase of soil. Linked to these phases, another one occupies the rest of the soil space. The combination of water and air constitutes it. Together, all these phases allow plant growth, limiting or favouring organisms' growth and the living matter on the soil [3]. There are several types of fertilizer. They are classified according to the number of nutrients they are made with, being so, fertilisers with a single nutrient or fertilisers with several types of nutrients. Fertilisers with several types of nutrients are classified into double nutrient

fertilisers, combining two necessary elements between Nitrogen (N), Phosphorus (P), or Potassium (K) [15].

Therefore, to perform the analysis of their phases, methods are traditionally used mainly based on chemical procedures, with extraction, digestion and processing samples, like colourimetry, for example [4]. Not so long ago, the use of sensors was an implemented idea with successful acceptance. They have the ability to transform physical or chemical readings from the environment into data signals, capable of being easily read by a system. Being said that, it is possible to place a large number of sensors around the study area so that they are capable of collecting data and sending it to a database. These sensors have two main purposes, monitoring the environment and tracking objects, animals, humans, etc. [5][6].

Typically, chemical methods are necessary for soil analysis. Nonetheless, they entail many associated disadvantages such as (i) high cost, (ii) long delay in order to obtain the results, (iii) use of reagents, and (iv) sample destruction [7]. Nowadays, sensors are able to determine soil fertility by taking measures of different parameters, such as soil pH, moisture, temperature, electrical conductivity, and nutrient levels. By giving these measures, it is possible to indicate whether applying any modification in the soil environment is necessary. Usually, sensors are able to provide relevant values regarding fertility, even in the presence of fertiliser [8]. The use of fertilisers allows an improvement in the physical soil properties and the numerous processes that the soil undergoes [9][10][11]. It is described, that a prolonged application and exposition to fertilisers, influence the quantity of solid matter [12], soil density, structure and ability to retain water [11][13][14]. When precision agriculture is applied to fertilizer application in drip irrigation yield increases by 22% [15].

The aim of the paper is to verify two sensors, one based on EM fields and the other based on optical effects, are better to determine the minimum fertiliser concentration necessary to optimise its use. For the EM-based sensor, we utilised a Two-Coil System (TCS) that used mutual inductance. A magnetic field was generated by the first coil that was powered with an alternate current (AC) source, thereby inducing a magnetic flux in the second non-powered coil or induced coil (IC). In order to determine which coil was best suited for this test, 4 different coils were tested, changing the spires numbers. A light source and a light

detector were used for the optical-based sensor. The fertiliser used was a liquid type with double nutrient composition, being that N and K. The main novelty of the proposed system is the combination of electromagnetic (EM) and optic sensors in a classification system so that it is possible to avoid overestimation of fertiliser. The system will save fertiliser, leading to economic savings for farmers.

The rest of the paper is structured as follows; Section 2 outlines the related work. The proposed system is fully described in Section 3. Following, Section 4 details the test bench. The results are discussed in Section 5. Finally, Section 6 summarises the conclusion and future work.

II. RELATED WORK

Currently, different types of sensors are being employed for the detection of fertilisers. For instance, visible/near-infrared (Vis/NIR) spectroscopy was reported to be effective in determining fertiliser content and reducing fertiliser waste by enabling more precise application of fertilisers by Lin et al. [16]. Similarly, a nitrogen-phosphorus-potassium (NPK) based sensor was developed by Lavanya et al. [17] for soil fertility monitoring. The proposed sensor worked on the colourimetric principle consisting of Light Dependent Resistor (LDR) and Light Emitting Diodes (LEDs).

In 2019 [18], the evaluation of the effects of irrigation and the application of mineral and organic fertiliser was proposed by mapping the variability of the apparent electrical conductivity using multiconfiguration electromagnetic induction. Deductions obtained by using this procedure showed that long-term fertiliser application influenced the electromagnetic induction measures and that multi-coil can be used to determine the homogeneity of agricultural treatments. According to Basterrechea, et al. [19] proposed measuring the quantity of organic fertiliser by using inductive coils. The results were rather conclusive, showing that one of their prototypes was valid.

Silva et al. [20] developed a novel procedure for detecting contaminants in water and organic fertilisers using portable and disposable commercial electrodes. They reported the use of electrochemical sensors efficient in detecting low concentrations of the substances in both water and organic fertilisers and postulated it an appropriate tool for environmental monitoring and quality control in agriculture.

Based on different approaches, Qiu and Qu [21] reported a novel non-enzymatic electrochemical sensor for the detection of nitrite derived from nitrogen fertilisers. This sensor was of polyaniline and manganese dioxide, a binary nanocomposite material. Further, it was demonstrated that electrochemical detection of nitrite is non-enzymatic and does not require the use of costly equipment. Recently, Meenakshi and Naresh [22] used crop image identification to analyse soil health and fertiliser requirement. The study utilised deep learning algorithms and random forest regression, and the results suggested that this image identification approach could be useful for precision agriculture and reducing fertiliser waste. Similar outcomes were found by Wang et al. [23] when they employed

machine vision technology to monitor the fertiliser use for corn fertiliser planters.

Nevertheless, all these currently employed fertiliser monitoring and estimation methods involve complex procedures in their employment, or data processing, or rely on a single parameter. Finally, some of the proposed solutions may require significant upfront investment or may not be financially viable for small-scale farmers, highlighting the need for cost-effective solutions. The system proposed in this paper is based on the combination of two parameters which can be measured using low-cost sensors. The use of two parameters reduces the possibility of overestimation due to irrigation water with elevated values of turbidity or salinity. The reasons to employ these sensors include their low cost, high accuracy, and easy deployment. In addition, promising results have been reported when similar sensors models were utilized in previous studies [18][24][25].

III. PROPOSAL

In this section, we detail the proposed system for fertiliser monitoring in irrigation systems. First, the EM and optical sensors are described. Then, the used node is characterised. Finally, the ANN model proposed for data classification is presented.

A. Sensor based on EM effects

Two pairs of inductive coils are tested to evaluate which TCS that offers the best results. Each pair of inductive coils can be used in two configurations by changing the powered and induced coil; more details are provided in the subsequent section. Since an alternating current is required to power the coil, a specific electronic circuit is included to power the coil using the microprocessor. The used circuit is fully described in [24].

The operational principle of EM-based sensors is that the presence of salts in the fertiliser modifies the induction of the induced coil, as demonstrated in [18]. Thus, it is expected that the V_{out} of the induced coil changes when the concentration of fertiliser is modified.

B. Sensor based on optical effects

The second included sensor in our proposed system is based on light absorption. Thus, a LED and a Light Dependent Resistor (LDR) are included. A microprocessor module, including an LDR, KY-018 [26], is used. As a light source, a white LED has been selected, which is powered by the microprocessor.

The optical-based sensors' operational principle is that the fertiliser's presence modifies the water's colour and transparency. It has a direct effect on light absorption. Therefore, it is expected a reduction in the light transmitted to the LDR, which modifies the received V_{out} in the microprocessor.

C. Node

A microprocessor is used to power the LED, the powered coil and the LDR and to receive the signal from the LDR and the induced coil. The selected microprocessor must accomplish the required analogue input for the coil and the

LDR module. In addition, it must be able to run an ANN model. Thus, a Raspberry Pi 4 Model B [27] is selected.

D. ANN model

The fact of using two sensors is to avoid false detection of fertiliser. If the induced coil is the single sensor, when fertiliser is added to water with moderate salinity values, as happened in some coastal areas, salinity might be considered as fertiliser. It will provoke an overestimation of fertiliser concentration. Thus, the optical sensor is used. The Artificial Neural Network (ANN) is selected to combine the data of both sensors. We have selected it since it can be easily implemented in the microprocessor. The proposed ANN can be seen in Figure 1.

IV. TEST BENCH

In this section, the complete test bench is detailed. First of all, sample preparation is described. Then, used sensors and their assemblage are detailed. The equipment used to feed the TCS is explained. Finally, the measurement procedure for data gathering and data analysis is presented.

A. Sample preparation

Six fertiliser calibration samples were prepared to create a calibration curve to identify the appropriate sensor model. A commercial organic fertiliser [28], containing nitrogen, phosphorous and other nutrients was used. The recommended dose is 10 mL of fertiliser mixed with 1 L of water. Therefore, in order to identify the lowest possible amount of fertiliser, six dilutions were prepared, see Table I. Each calibration sample has a volume of 500 mL. The volumes used for the calibration include 100 mL.

B. TCS description

Two TCSs, TCS 1 and TCS 2, which can be connected in four configurations, were employed in these tests. TCSs can be seen in Figure 2a and Figure 2b.

The TCSs can be connected in two different configurations (a and b) since they have different spires. The number of spires in the IC and the PC of each configuration of the used TCSs are summarised in Table II. The wire used to craft the coils was enamelled copper coil of 0.4 mm diameter. These coils were wrapped on a 25 mm diameter Polyvinyl chloride (PVC) tube with an empty core.

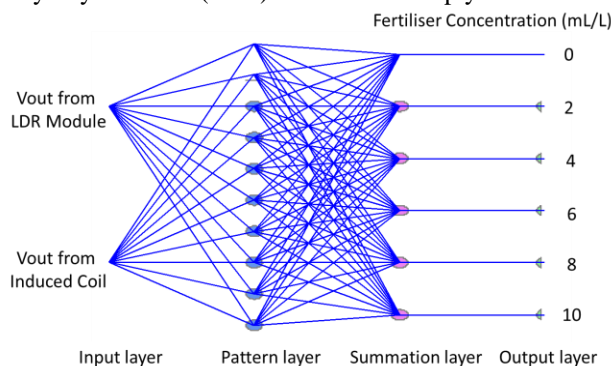


Figure 1. Proposed ANN model.

TABLE I. FERTILISER SAMPLES

Sample No	Sample content		
	Added Fertiliser	Added Water	Dose (mL/L)
1	0	500	0
2	1	499	2
3	2	498	4
4	3	497	6
5	4	496	8
6	5	495	10

TABLE II. SUMMARY OF TCSs' CHARACTERISTICS

Sample No	Features			
	Number of spires		Diameter (mm)	
	IC	PC	Coil	PVC Tube
TCS 1 a	80	40	0.4	25
TCS 1 b	40	80	0.4	25
TCS 2 a	40	20	0.4	25
TCS 2 b	20	40	0.4	25

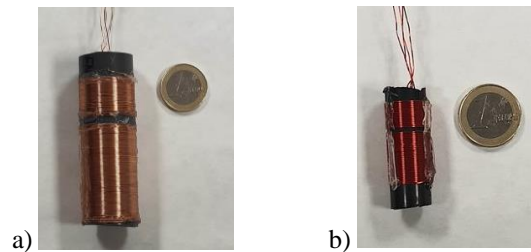


Figure 2. Used TCSs a) TCS 1, b) TCS 2.

C. Optical sensor assemblage

The measures were taken by connecting the LDR module to the microprocessor. The LED and the LDR were separated 3 cm by a methacrylate transparent tube. The tube was filled with the calibration samples. The Vout from the LDR module was obtained from the microprocessor using the analogue input.

D. Equipment

A wave generator, model AFG1022 [29], has been used to power the PC. Resistance of 330 Ω was connected in series to PC. A sine wave having an amplitude of 3.3 V peak-to-peak and 0.045 A have been used to power the coils. The used signal generator allows a range of frequencies from 25 MHz to 1 uHz.

The IC is connected to an oscilloscope, model TBS1104 [30]. A capacitor of 10 nF was added in parallel to the IC. The complete scheme of the used devices and the electronic circuit can be seen in Figure 3.

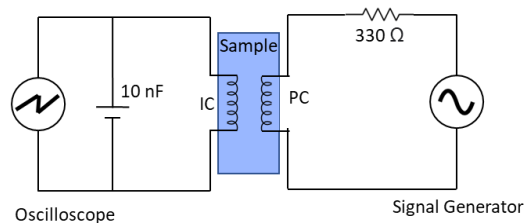


Figure 3. TCS circuit.

E. Measurement protocol and data analysis

The measurement protocol followed for the calibration process consists of measuring the V_{out} values of the TCS or the LDR module. Measurements started from the most diluted samples, sample 1, to the most concentrated one, sample 6. Each measurement was repeated three times.

In the TCS measurement procedure, the oscilloscope is used to gather the data as a previous step before adapting the required electronic circuit to measure it with the microprocessor. The first step is to identify the working frequency for each used PC. Once the working frequency is determined, calibration starts. For the calibration, the TCS was entirely submerged in the calibration samples. Induced voltage, V_{out} , was gathered individually for all used sensors.

For the optical-based sensors, the measurement procedure consists of adding fertiliser inside the methacrylate tube. Then, the white LED is powered by the microprocessor. At the same time, the microprocessor reads the value from the analogue input of the LDR module.

Obtained data is statistically analysed. The performed analyses include descriptive statistics, simple regression models and Discriminant analyses (DA). All these analyses, in addition to the ANN, have been performed with the Statgraphics Centurion XVIII.

V. RESULTS

In this section, we present the results from the obtained V_{out} from both sensors. First, the results of the descriptive statistics are shown for the V_{out} of the induced coil to decide which coil and configuration are selected. Then, the results of the mathematical models are compared. Finally, the results of the ANN are analysed.

A. Descriptive statistics of V_{out} from induced coils

First of all, the working frequencies are presented. The working frequency for the used TCSs was: 147 kHz for TCS 1 a, 267 kHz for the TCS 1 b, 433 kHz for TCS 2 a, and 665 kHz for the TCS 2b.

The summation of descriptive analyses of data from IC can be seen in Table III. The Table shows that the coil that maximises the average V_{out} is TCS 1 a. TCS 1 b is characterised by a mean V_{out} of 2.52 V, which is similar to the mean V_{out} of TCS 2 b, 2.21 V. TCS 1 b is the one with lowers mean V_{out} , 1.88 V. The standard deviation (σ) is the minimum for TCS 2 a and TCS 2 b. Finally, values of Kurtosis and Skewness are between ± 2 for TCS 1 b, 2a, and 2b. Nonetheless, for TCS 1 a, the values are beyond the

established thresholds to be considered a variable with normal distribution.

Finally, Figure 4 portrays the distribution of each variable as violin plots. For these plots, cosine has been used as a smoothing method. The interval width has been set at 35. The means and outliers are represented in the graphic.

B. Simple Regression Models

In this section, the single correlation models for each one of the EM-based sensors are presented. The regression models were selected among the available options, maximising the correlation coefficient's value. The summary of regression models can be seen in Table IV. In the table, the selected model type, the correlation coefficient and the R-squared (R^2). According to the R^2 and correlation coefficients, we selected TCS 1 a and TCS 2 b as two alternatives for EM-based sensors for the proposed system.

The correlation models for TCS 1 a and TCS 2 b can be seen in Figure 5 and Figure 6, respectively. The mathematical model represents confidence and prediction intervals in both figures. We selected the second model for the obtained models due to their more accurate intervals. Moreover, the first option, inducer 1 a, has maximum values which are too high for the analogue inputs for the microprocessor.

C. Classification Methodologies

Finally, we combine the data for the V_{out} from the TCS 2 b and the LDR module for the classification methods. On the one hand, the classification diagram for the DA based on generated functions can be seen in Figure 7. On the other hand, the classification diagram for the ANN can be seen in Figure 8. For the ANN, the dataset was split into a training dataset (first and second replicas of tests) and a validation dataset (third replica). Regarding the classified cases, both tested classification methods, DA and ANN, allow the classification of 100% of cases.

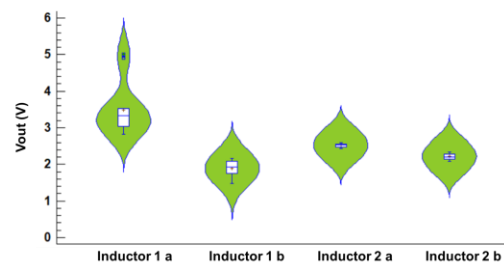


Figure 4. Violin plot of V_{out} for the different sensors.

TABLE III. SUMMARY OF CHARACTERISTICS OF THE SELECTED JELLYFISH

	Sensor 1		Sensor 2	
	TCS 1 a	TCS 1 b	TCS 2 a	TCS 2 b
Mean V_{out} (V)	3.49556	1.88444	2.52778	2.21333
Minimum V_{out} (V)	2.82	1.48	2.44	2.08
Maximum V_{out} (V)	5	2.16	2.6	2.34
σ	0.713914	0.226747	0.0470988	0.0840168
Kurtosis	2.58232	-0.963285	-0.807876	-0.165955
Skewness	0.94211	-0.763609	-0.781795	-1.12133

TABLE IV. SUMMARY OF TCSS' CHARACTERISTICS

TCS	Selected model	Correlation coefficient	R ²
TCS 1 a	$Y = 1/(a + b*\sqrt{X})$	0.987	97.45
TCS 1 b	$Y = \sqrt{a + b*X}$	-0.822	67.638
TCS 2 a	$Y = \sqrt{a + b*\sqrt{X}}$	-0.312	9.725
TCS 2 b	$Y = \sqrt{a + b*X}$	0.988	97.709

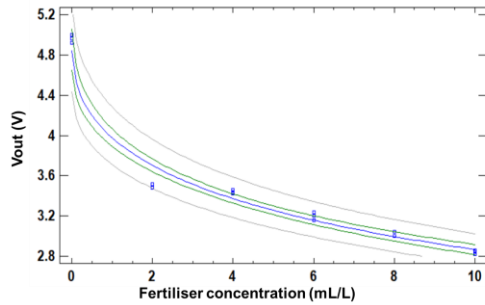


Figure 5. X-Y Plot for Vout of the TCS 1 a.

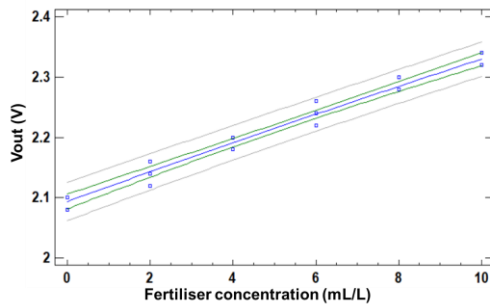


Figure 6. X-Y Plot for Vout of the TCS 2 b.

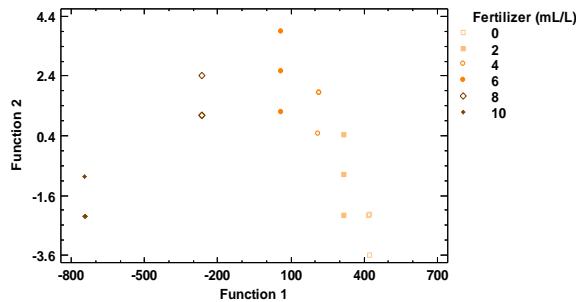


Figure 7. Classification diagram with DA.

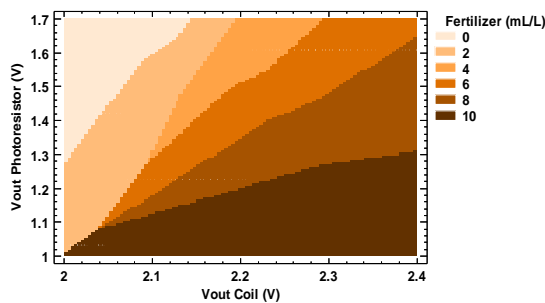


Figure 8. Classification diagram with ANN.

In both training and validation, 100 % of correctly classified cases were attained. A second classification was done by selecting the data for each dataset randomly, with the same percentage of cases correctly classified in both the training and validation dataset.

VI. CONCLUSIONS AND FUTURE WORK

The use of fertiliser has increased considerably in recent years. The need to produce food in the shortest possible time and protect the fruit against biological agents has become a current area of research.

In this paper, we presented a system for optimising liquid fertilisers for irrigation water. The system is based on TCSS that generate electromagnetic fields that allow the establishment of the concentrations of fertilisers. Thus, Vout measurements are established for each solution prepared. A function generator has been used and visualised in an oscilloscope to generate the electromagnetic field. In addition, an LDR and a photoresistor have been implemented to obtain data to avoid overestimating the fertiliser concentration. After applying the statistical analysis, the results show that the system can classify 100% fertiliser solutions with different concentrations.

In future work, we want to maximise the sensitivity of the coil at smaller concentrations and check in a real environment how the decrease in fertiliser does not affect plant growth. This fact would allow economic savings for the farmer, as well as a decrease in the use of products in agriculture.

ACKNOWLEDGMENT

This work has been funded by the “Ministerio de Ciencia e Innovación” through the Project PID2020-114467RR-C33/AEI/10.13039/501100011033, by “Ministerio de Agricultura, Pesca y Alimentación” through the “proyectos de innovación de interés general por grupos operativos de la Asociación Europea para la Innovación en materia de productividad y sostenibilidad agrícolas (AEI-Agri)”, project GO TECNOGAR, and by the “Ministerio de Economía y Competitividad” through the Project TED2021-131040B-C31. This study also forms part of the ThinkInAzul programme and was supported by MCIN with funding from European Union NextGenerationEU (PRTR-C17.I1) and by Generalitat Valenciana (THINKINAZUL/2021/002).

REFERENCES

- [1] A. Desbiez, R. Matthews, B. Tripathi, and J. EllisJones, “Perceptions and assessment of soil fertility by farmers in the mid-hills of Nepal,” *Agric. Ecosyst. Environ.*, vol. 103, no. 1, pp. 191–206, 2004.
- [2] I. M. Cardoso and T. W. Kuyper, “Mycorrhizas and tropical soil fertility,” *Agric. Ecosyst. Environ.*, vol. 116, no. 1–2, pp. 72–84, 2006.
- [3] N. Uphoff et al., “Biological Approaches to Sustainable Soil Systems,” *Books in ScienceBiol. Approaches to Sustain. Soil Syst.*, no. Jan., 2006.
- [4] N.T. Fainthfull NT, “Methods in agricultural chemical analysis,” CABI Publishing, Oxfordshire, pp 57–104, 2002.

- [5] J. Yick, B. Mukherjee, and D. Ghosal, "Wireless sensor network survey," *Comput. Networks*, vol. 52, no. 12, pp. 2292–2330, 2008.
- [6] J. Lloret, M. Garcia, F. Boronat, and J. Tomás, "A group-based protocol for large wireless AD-HOC and sensor networks," 2008 IEEE Netw. Oper. Manag. Symp. Work. - NOMS 08, vol. 23, no. May, pp. 7–14, 2008.
- [7] E. Lopez and F. Miñano, "Metodos rapidos de analisis de suelos," *Minist. Agric. Pesca y Aliment.*, p. 32pp, 2008.
- [8] S. Postolache, P. Sebastião, V. Viegas, O. Postolache, and F. Cercas, "IoT-Based Systems for Soil Nutrients Assessment in Horticulture," *Sensors*, vol. 23, no. 1, 2023.
- [9] D. W. Reeves, "The role of soil organic matter in maintaining soil quality in continuous cropping systems," *Soil Tillage Res.*, vol. 43, no. 1–2, pp. 131–167, 1997.
- [10] B. J. Zebarth, G. H. Neilsen, E. Hogue, and D. Neilsen, "Influence of organic waste amendments on selected soil physical and chemical properties," *Can. J. Soil Sci.*, vol. 79, no. 3, pp. 501–504, 1999.
- [11] I. Celik, I. Ortas, and S. Kilic, "Effects of compost, mycorrhiza, manure and fertilizer on some physical properties of a Chromoxerert soil," *Soil Tillage Res.*, vol. 78, no. 1, pp. 59–67, 2004.
- [12] D. K. Benbi, C. R. Biswas, S. S. Bawa, and K. Kumar, "Influence of farmyard manure, inorganic fertilizers and weed control practices on some soil physical properties in a long-term experiment," *Soil Use Manag.*, vol. 14, no. 1, pp. 52–54, 1998.
- [13] J. J. Miller, N. J. Sweetland, and C. Chang, "Hydrological Properties of a Clay Loam Soil after Long-Term Cattle Manure Application," *J. Environ. Qual.*, vol. 31, no. 3, pp. 989–996, 2002.
- [14] P. Schjøning, L. J. Munkholm, P. Moldrup, and O. H. Jacobsen, "Modelling soil pore characteristics from measurements of air exchange: The long-term effects of fertilization and crop rotation," *Eur. J. Soil Sci.*, vol. 53, no. 2, pp. 331–339, 2002.
- [15] Shareef, T. M. E., Ma, Z., & Zhao, B., "Essentials of drip irrigation system for saving water and nutrients to plant roots: As a guide for growers." *Journal of Water Resource and Protection.*, Vol 11, no 9, pp. 1129-1145, 2019.
- [16] Z. Lin et al., "Accurate and rapid detection of soil and fertilizer properties based on visible/near-infrared spectroscopy," *Applied Optics*, vol. 57, no. 18, pp. D69-D73, 2018.
- [17] G. Lavanya, C. Rani, and P. GaneshKumar, "An automated low cost IoT based Fertilizer Intimation System for smart agriculture," *Sustainable Computing: Informatics and Systems*, vol. 28, p. 100300, 2020.
- [18] J. Nie et al., "Effect of drip irrigation with magnetized water and fertilizer on cotton nutrient absorption." *IOP Conference Series: Earth and Environmental Science*. vol. 697. no. 1, IOP Publishing, 2021.
- [19] D. A. Basterrechea, L. Parra, M. Botella-Campos, J. Lloret, and P. V. Mauri, "New Sensor Based on Magnetic Fields for Monitoring the Concentration of Organic Fertilizers in Fertigation Systems," *Applied Sciences*, vol. 10, no. 20, p. 7222, Oct. 2020.
- [20] L. R. Silva, J. G. Rodrigues, M. de LS Vasconcellos, E. S. Ribeiro, E. D'Elia, and R. de Q. Ferreira, "Portable and simple electroanalytical procedure for simultaneous detection of dipyrone and norfloxacin with disposable commercial electrodes in water and organic fertilisers," *Ionics*, vol. 28, no. 10, pp. 4833-4841, 2022.
- [21] Y. Qiu and K. Qu, "Binary organic-inorganic nanocomposite of polyaniline-MnO₂ for non-enzymatic electrochemical detection of environmental pollutant nitrite," *Environmental Research*, vol. 214, p. 114066, 2022.
- [22] M. Meenakshi and R. Naresh, "Soil health analysis and fertiliser prediction for crop image identification by Inception-V3 and random forest," *Remote Sensing Applications: Society and Environment*, vol. 28, p. 100846, 2022.
- [23] B. Wang, Y. Wang, H. Wang, H. Mao, and L. Zhou, "Research on accurate perception and control system of fertilisation amount for corn fertilisation planter," *Frontiers in Plant Science*, vol. 13, no. 1074945, 2022.
- [24] L. Parra, S. Viciano-Tudela, D. Carrasco, S. Sendra, and J. Lloret, "Low-Cost Microcontroller-Based Multiparametric Probe for Coastal Area Monitoring," *Sensors*, vol. 23, no. 4, 2023.
- [25] Y. Wang, S. S. M. Rajib, C. Collins, and B. Grieve, "Low-cost turbidity sensor for low-power wireless monitoring of fresh-water courses," *IEEE Sensors Journal*, vol. 18, no. 11, pp. 4689-4696, 2018.
- [26] LDR module . KY-018. Available online: https://datasheet.lcsc.com/szlcsc/Shenzhen-Jing-Chuang-He-Li-Tech-GL5528-10-20_C10081.pdf. (accessed on 23 February 2023).
- [27] Raspberry Pi 4 Model B. Available online: <https://datasheets.raspberrypi.com/rpi4/raspberry-pi-4-datasheet.pdf> (accessed on 23 February 2023).
- [28] Fertilizer Datasheet. Available at: https://www.compo.de/dam/jcr:e4246087-ca92-4ea5-83da-52aa203e1d42/2224501004_r0427195.PDF [Last access on 23/02/2023]
- [29] Information of the current generator used. Available at: <https://www.mouser.com/datasheet/2/403/AFG1022-Arbitrary-Function-Generator-Datasheet-1-540840.pdf> [Last access on 23/02/2022].
- [30] Information of the Oscilloscope used. Available at: <https://www.mouser.com/datasheet/2/403/AFG1022-Arbitrary-Function-Generator-Datasheet-1-540840.pdf> [Last access on 23/02/2022].